FUDMA Journal of Sciences (FJS)
ISSN online: 2616-1370
ISSN print: 2645 - 2944
Vol. 10 No. 5, March, 2026, pp 183 – 196
DOI: https://doi.org/10.33003/fjs-2026-1005-4987

STRUCTURE-BASED DISCOVERY OF ABSCISIC ACID RECEPTOR AGONISTS TARGETING ZMPYL9 AND ZMPYL12 FOR AGROCHEMICAL DEVELOPMENT

***[1]Ayinla, AbdulAziz., [1]Ibrahim, S. Ahmad, [1]Opadokun, O. Wasiu, [2]Olayinka, B. Umar, [3]Lawal, R. Amudalat, [1]Balogun, AbdulAzeez., [1]Koiki, O. AbdulRasheed, [1]Alao, A. Quam, and [1]Oyelekan, A. Sunday**

[1]Department of Biological Sciences, Al-Hikmah University, Ilorin, Kwara State, Nigeria.
[2]Department of Plant Biology, University of Ilorin, Kwara State, Nigeria.
[3]Department of Plant and Environmental Biology, Kwara State University Malete, Kwara State, Nigeria.

*Corresponding authors' email: aayinla@alhikmah.edu.ng Phone: +2347033906219

ABSTRACT

Abiotic stress, particularly drought, remains a major limitation to crop productivity, necessitating innovative strategies to enhance plant resilience. Abscisic acid (ABA) signalling, mediated by PYR/PYL/RCAR receptors, plays a central role in stress adaptation; however, structural and functional insights into specific maize receptors such as ZmPYL9 and ZmPYL12 remain limited. This study employed an integrated computational approach to characterize these receptors and identify potential ABA-mimicking agrochemicals. High-quality homology models of ZmPYL9 and ZmPYL12 were constructed using templates with >94% sequence identity, yielding structurally robust models validated by stereochemical and non-bonded interaction metrics. Pharmacophore modelling and molecular docking revealed key ligand-binding features consistent with the canonical gate-latch-lock activation mechanism. Several compounds exhibited strong binding affinities (≤ −10 kcal/mol), while MM-GBSA analysis identified compounds 10661840 (−96.18 kcal/mol) and 10588337 (−93.21 kcal/mol) as the most stable ligands for ZmPYL9, and compound 134611692 (−94.73 kcal/mol) for ZmPYL12. Drug-likeness evaluation confirmed compliance with agrochemical criteria, while ADMET profiling indicated high bioavailability, low metabolic interference, and minimal toxicity. Notably, ZmPYL9 demonstrated superior ligand-binding performance, suggesting greater suitability for targeted modulation. This study therefore provide novel insights into receptor-specific ligand interactions and establishes a robust structure-based framework for the rational design of ABA agonists. The identified lead compounds represent promising candidates for developing environmentally safe agrochemicals aimed at improving crop tolerance to abiotic stress.

Keywords: Abscisic Acid (ABA); PYR/PYL/RCAR Receptors; Zmpyl9; Zmpyl12; Homology Modelling; MM-GBSA; Ligand Binding Affinity; Agrochemical Design; Plant Stress Tolerance

INTRODUCTION

Abiotic stress remains one of the most significant constraints on global crop productivity, particularly in the context of climate change–induced drought and temperature variability. Among the key hormonal regulators of plant stress responses, abscisic acid (ABA) plays a central role in mediating physiological and molecular adaptations, including stomatal closure, osmotic adjustment, and stress-responsive gene expression (Melcher et al., 2009; Sah et al. 2016; Sharma & Sharma, 2023). The perception and transduction of ABA signals are primarily governed by the pyrabactin resistance1/pyr1-like/regulatory components of aba receptors (PYR/PYL/RCAR) protein family, which function as intracellular receptors that initiate downstream signalling cascades through inhibition of type 2C protein phosphatases (PP2Cs) (Park et al., 2009; Fidler et al., 2022).

In crops such as maize (*Zea mays* L.), ABA signalling is critically important for adaptation to water-deficit conditions, yet the structural and functional characterization of individual ABA receptor isoforms remains incomplete. Among these, ZmPYL9 and ZmPYL12 are putative ABA receptors that are presumed to contribute to stress tolerance; however, their structural properties, ligand-binding mechanisms, and potential for agrochemical targeting have not been fully elucidated. Given the high degree of conservation within the PYR/PYL/RCAR family, computational approaches such as homology modelling and structure-based ligand design provide a powerful framework for predicting receptor structure and function with high accuracy, particularly when suitable templates with high sequence identity are available (Waterhouse et al., 2018; Bienert et al., 2017).

Recent advances in structural biology, including high-resolution X-ray crystallography and machine learning–based prediction tools such as AlphaFold, have significantly enhanced the reliability of *in silico* protein modelling. These approaches enable detailed investigation of ligand-induced conformational dynamics, particularly the conserved gate-latch-lock mechanism that underpins ABA receptor activation (Melcher et al., 2009; Sah et al. 2016; Sharma & Sharma, 2023). Importantly, the availability of ligand-bound receptor structures provides critical insights into the molecular determinants of binding specificity and affinity, facilitating the rational design of ABA analogues with improved efficacy. The development of synthetic ABA agonists represents a promising strategy for enhancing plant stress tolerance and agricultural resilience. However, successful agrochemical design requires not only strong receptor binding but also favourable physicochemical, pharmacokinetic, and toxicological properties to ensure efficacy, environmental safety, and regulatory compliance (Tice, 2001; Driver et al., 2020). In this context, integrated computational pipelines combining pharmacophore modeling, molecular docking, binding free energy calculations, and ADMET prediction have emerged as essential tools for identifying and optimizing bioactive compounds (Daina et al., 2017; Pires et al., 2015). Despite these advances, there remains a critical need to identify receptor-specific ligand interactions and to evaluate the suitability of candidate compounds for plant-targeted applications. In particular, comparative analysis of different PYL isoforms may reveal subtle structural variations that influence ligand selectivity, binding affinity, and downstream signalling efficiency. Therefore, the present study aimed to (i)

construct and validate high-quality homology models of ZmPYL9 and ZmPYL12, (ii) characterize their ligand-binding properties through pharmacophore modeling and molecular docking, (iii) evaluate binding stability using MM-GBSA free energy analysis, and (iv) assess the agrochemical potential of identified compounds through drug-likeness, ADMET, and toxicity profiling. By integrating structural bioinformatics with ligand discovery approaches, this study provides novel insights into ABA receptor functionality in maize and establishes a robust computational framework for the rational design of ABA-mimicking agrochemicals for improved stress resilience.

MATERIALS AND METHODS

Sequence Retrieval and Template Selection

The amino acid sequences of ZmPYL9 and ZmPYL12 were retrieved from NCBI online repositories. Homologous structural templates were identified using BLASTp against the Protein Data Bank (PDB), with selection criteria based on sequence identity (>90%), query coverage (>80%), and availability of ligand-bound conformations. High-resolution X-ray crystal structures and AlphaFold-derived models were included to ensure accurate structural representation of receptor conformations relevant to ligand binding.

Homology Modelling and Structure Validation

Three-dimensional models were generated using the SWISS-MODEL server, which employs evolutionary information to construct reliable protein structures (Waterhouse et al., 2018; Studer et al., 2020). Model quality was assessed using Global Model Quality Estimation (GMQE) and QMEANDisCo scores. Structural validation was performed using MolProbity for stereochemical evaluation, PROCHECK for Ramachandran plot analysis, and ERRAT for non-bonded interaction quality assessment. Models exhibiting optimal geometric integrity and minimal steric clashes were selected for downstream analyses.

Pharmacophore Modelling and Virtual Screening

Structure-based pharmacophore models were developed from ABA-bound receptor complexes by identifying key interaction features, including hydrogen bond donors/acceptors, hydrophobic regions, and aromatic interactions. Virtual screening was conducted using PubChem-derived compound libraries under both ligand-receptor shape-constrained and unconstrained conditions to maximize identification of structurally diverse ABA analogues.

Molecular Docking Analysis

Molecular docking was performed using AutoDock Vina to evaluate ligand-receptor interactions. Protein structures were prepared by removing water molecules and adding polar hydrogens, while ligands were energy-minimized prior to docking. Binding affinities were expressed as docking scores (kcal/mol), and binding poses were analysed to identify key residues involved in ligand stabilization.

Binding Free Energy Calculations

The stability of ligand-receptor complexes was further evaluated using Molecular Mechanics Generalized Born Surface Area (MM-GBSA) calculations, which provide improved estimation of binding free energy by incorporating solvation effects and entropic contributions.

Drug-Likeness and ADMET Prediction

Physicochemical and pharmacokinetic properties were evaluated using SwissADME and pkCSM web servers. These tools enable prediction of absorption, distribution, metabolism, excretion, and toxicity (ADMET) parameters, as well as drug-likeness descriptors critical for lead optimization (Daina et al., 2017; Al Azzam et al., 2022). Key parameters assessed included gastrointestinal absorption, cytochrome P450 inhibition, P-glycoprotein interaction, and lipophilicity.

Toxicity Assessment

Toxicological profiles, including mutagenicity, carcinogenicity, cytotoxicity, immunotoxicity, and acute toxicity (LD_{50}), were predicted using *in silico* toxicity platforms such as ProTox-II and pkCSM. Compounds with favourable safety profiles were prioritized for further consideration as potential agrochemical candidates.

RESULTS AND DISCUSSION

Homology Modelling and Template Selection

The selection of structural templates for ZmPYL9 and ZmPYL12 revealed exceptionally high sequence identity (94–100%) and substantial coverage of ~0.81–1.00 (Tables 1 and 2), indicating strong evolutionary conservation within the PYR/PYL/RCAR abscisic acid (ABA) receptor family. High sequence identity above 50% is widely associated with accurate homology modelling, while values exceeding 90% typically yield near-experimental structural fidelity (Waterhouse et al., 2018; Bienert et al., 2017). The inclusion of both experimentally resolved X-ray crystal structures (2.1–2.6 Å) and AlphaFold-derived models ensured comprehensive conformational sampling, particularly in ligand-bound states relevant for functional interpretation. Notably, the presence of templates co-crystallized with ABA and pyrabactin is critical, as ligand-induced conformational changes especially in the gate-latch region define receptor activation and downstream signalling (Melcher et al., 2009; Sharma & Sharma, 2023). Thus, template selection provided a structurally and functionally relevant foundation for downstream modelling.

Table 1: Structural Templates Selected For Zmpyl9 Homology Modelling

Model No	ID	Coverage	Sequence identity (%)	Sequence Similarity	GMQE	QSQE	Method and Resolution	Ligand
1.	B4FVL9.1.A	1.00	100	0.62	0.87	-	AlphaFold v2	None
2.	5zcu.1.B	0.83	97.14	0.61	0.76	-	X-ray, 2.4Å	Pyrabactin
3.	5zch.2.B	0.83	97.14	0.61	0.75	-	X-ray, 2.5Å	ABA
4.	5gwp.1.B	0.83	97.14	0.61	0.75	-	X-ray, 2.6Å	ABA
5.	5zcu.1.B	0.82	97.11	0.61	0.75	-	X-ray, 2.4Å	Pyrabactin

Table 2: Structural Templates Selected For Zmpyl12 Homology Modelling

Model No	ID	Coverage	Sequence identity (%)	Sequence Similarity	GMQE	QSQE	Method and Resolution	Ligand
1.	B4FVL9.1.A	1.00	100	0.62	0.87	-	AlphaFold v2	None
2.	5zcu.1.B	0.83	97.14	0.61	0.76	-	X-ray, 2.4Å	Pyrabactin
3.	5zch.2.B	0.83	97.14	0.61	0.75	-	X-ray, 2.5Å	ABA
4.	5gwp.1.B	0.83	97.14	0.61	0.75	-	X-ray, 2.6Å	ABA
5.	5zcu.1.B	0.82	97.11	0.61	0.75	-	X-ray, 2.4Å	Pyrabactin

Structural Validation and Model Reliability

For ZmPYL9, all generated models demonstrated acceptable global folding quality (GMQE ~0.71–0.72; QMEANDisCo ~0.85), confirming consistency in structural prediction (Table 3). However, Model 5 (based on template 5zcg.1.B) exhibited superior stereochemical quality, with the lowest MolProbity score (0.74), minimal steric clashes (0.77), and the highest proportion of Ramachandran favoured residues (98.73%) without outliers (Table 3). These metrics indicate optimal backbone geometry and reduced conformational strain. Further validation using ERRAT identified Models 3 and 5 as acceptable with values >95% (Table 5), with Model 5 selected due to its superior stereochemical profile. High ERRAT scores are indicative of reliable non-bonded atomic interactions, reinforcing the structural integrity of the model (Colovos & Yeates, 1993; Tian et al., 2018). Although all ZmPYL12 models exhibited high stereochemical quality (>96% Ramachandran favoured residues), ERRAT validation identified only Model 4 (99.32%) as acceptable (Table 5). This suggests that subtle differences in non-bonded interactions, rather than backbone geometry alone, determine structural reliability. The selected model therefore represents the most accurate conformation for ligand-binding studies. Collectively, these results confirm that both ZmPYL9 and ZmPYL12 models are structurally robust, with ZmPYL9 Model 5 (Figure 1) and ZmPYL12 Model 4 (Figure 2) selected for downstream analyses.

Table 3: SWISS-Model Structural Assessment for Zmpyl9

					MolProbity Results									
Model No.	Template ID	GMQE	QMEANDisCO Global	QMEAN	MolProbity Score	Clash Score	R Favored	R Outliers	R. Outliers	c-Beta Deviations	Bad Bonds	Bad Angles	Cis Non-Proline	Twisted Non-Proline
1.	B4FD84.1.A	-	-	-	1.05	0.59	94.88%	0.47%	0.53%	0	0 / 1738	23 / 2355	1 / 202	3 / 202
2.	5zcu.1.B	0.71	0.85±0.07	0.05	0.95	1.91	98.12%	0.00%	0.00%	1	0 / 1319	24 / 1785	-	-
3.	5gwp.1.B	0.72	0.86±0.07	-0.03	1.09	1.53	96.86%	.00%	0.00%	1	1 / 1312	24 / 1775	-	-
4.	5zch.2.B	0.72	0.85±0.07	-0.21	1.11	1.13	96.89%	0.00%	1.35%	0	0 / 1327	22 / 1795	1 / 154	-
5.	5zcg.1.B	0.71	0.86±0.07	0.15	0.74	0.77	98.73%	0.00%	0.69%	0	1 / 1301	21 / 1761	-	-

Table 4: SWISS-Model Structural Assessment for Zmpyl12

					MolProbity Results									
Model No.	Template ID	GMQE	QMEANDisCO Global	QMEAN	MolProbity Score	Clash Score	R Favored	R Outliers	R. Outliers	c-Beta Deviations	Bad Bonds	Bad Angles	Cis Non-Proline	Twisted Non-Proline
1.	B4FVL9.1.A	0.87	-	-	0.77	0.30	97.14	0.00	0.54	1	0/1709	14/2309	-	-
2.	5zcu.1.B	0.73	0.85±0.07	0.45	0.95	1.90	98.75	0.00	0.00	1	0 / 1324	19 / 1792	-	-
3.	5zch.2.B	0.73	0.85 ± 0.07	0.13	1.09	1.50	97.52%	0.00	1.34	1	1 / 1333	21 / 1803	1 / 154	-
4.	5gwp.1.B	0.73	0.86±0.07	0.36	1.02	1.14	96.86	0.00	0.00	1	1 / 1317	24 / 1782	-	-
5.	5zcu.1.B	0.73	0.85 ± 0.07	0.45	0.95	1.90	98.75	0.00	0.00	1	0 / 1324	19 / 1792		

Table 5: Errat Validation for Zmpyl9 and Zmpyl12

S/N	Protein Receptor	Models	Overall Quality Factor (%)	Remark
1	ZmPYL9	1	87.5676	Rejected
		2	93.007	Rejected
		3	100	Accepted
		4	92.3077	Rejected
		5	95.9184	Accepted
2	ZmPYL12	1	91.8033	Rejected
		2	93.1034	Rejected

S/N	Protein Receptor	Models	Overall Quality Factor (%)	Remark
		3	93.007	Rejected
		4	99.3197	Accepted
		5	93.1034	Rejected

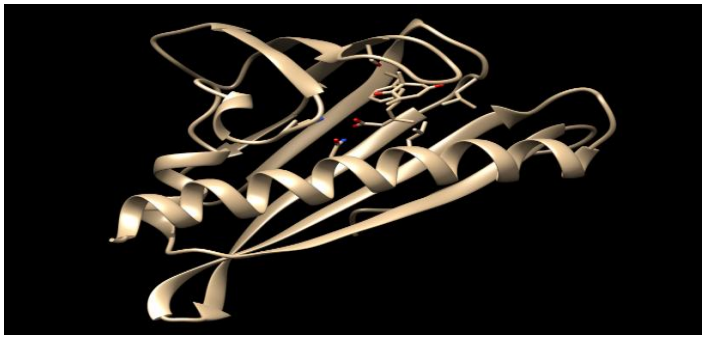

Figure 1: Model 5 – ZmPLY9 Homology Protein Structural Representation in Complex with Abscisic Acid

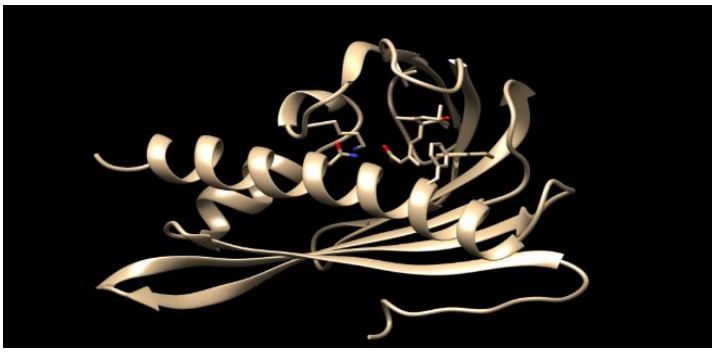

Figure 2: Model 4 – ZmPLY12 Homology Protein Structural Representation in Complex with Abscisic Acid

Pharmacophore Modelling and Ligand Binding Characteristics

Pharmacophore modelling based on abscisic acid (ABA)-bound complexes revealed key interaction features consistent with the canonical ABA receptor mechanism. Under ligand and receptor shape constraints, ZmPYL9 generated a limited set of four pharmacophore models with binding affinities around −9.46 kcal/mol and low RMSD of ~0.55 (Table 6), indicating high conformational consistency and precise alignment with the ABA-binding pocket. In contrast, removal of shape constraints significantly expanded chemical diversity, yielding compounds with improved binding affinities (up to −10.45 kcal/mol). This highlights a trade-off between structural specificity and ligand diversity, where relaxed constraints facilitate identification of high-affinity analogues beyond strict ABA mimicry. Notably, unconstrained pharmacophore screening enabled the identification of several high-affinity candidates, including PubChem compounds 15479571 and 166176980, which exhibited docking scores below −10 kcal/mol (Table 7). However, further integration with binding free energy calculations revealed that compounds such as 10661840, 10588337, and 10379033 demonstrated superior thermodynamic stability, with MM-GBSA values reaching −96.18, −93.21, and −92.31 kcal/mol, respectively. These findings emphasize the importance of combining pharmacophore modelling with post-docking refinement to accurately prioritize lead compounds.

Mechanistically, these observations align with the gate-latch-lock model of ABA receptor activation, in which ligand binding induces conformational closure of conserved loops that stabilize receptor–PP2C interactions (Park et al., 2009; Sah et al. 2016; Sharma & Sharma, 2023). The identification of ABA-like compounds with enhanced binding stability suggests potential for stronger or prolonged receptor activation. ZmPYL12 exhibited a similar but slightly reduced binding affinity range (maximum ~−9.79 kcal/mol), consistent with the identification of compound 134611692 as the most stable ligand with MM-GBSA value of −94.73 kcal/mol (Table 8). This reduced affinity spectrum suggests subtle differences in binding pocket flexibility or residue composition, supporting previous reports that individual PYL receptors display distinct ligand selectivity despite structural conservation (Fidler et al., 2022).

Table 6: Zmply9 Models with both Ligand and Receptor Shape Restrictions

S/N	Pubchem ID	Compound Name	SMILEs	Minimized affinity (kcal/mol)	Minimized RMSD
1	14702801	(2Z,4E)-5-[(1S,6S)-1-hydroxy-2,2,6-trimethyl-4-oxocyclohexyl]-3-methylpenta-2,4-dienoic acid	C[C@H]1CC(=O)CC([C@]1(/C=C/C(=C\C(=O)O)/C)O)(C)C	-9.46833	0.55092
2	141780114	(2Z,4E)-5-[(1S)-1-hydroxy-2,2,6-trimethyl-4-	CC1CC(=O)CC([C@]1(/C=C/C(=C\C(=O)O)/C)O)(C)C	-9.46221	0.56173

S/N	Pubchem ID	Compound Name	SMILEs	Minimized affinity (kcal/mol)	Minimized RMSD
		oxocyclohexyl]-3-methylpenta-2,4-dienoic acid			
3	141812992	(2Z,4E)-5-(1-hydroxy-2,2,6-trimethyl-4-oxocyclohexyl)-3-methylpenta-2,4-dienoic acid	CC1CC(=O)CC(C1(/C=C/C(=C\C(=O)O)/C)O)(C)C	-9.46219	0.56172
4	101949275	(2Z,4E)-5-[(6S)-1-hydroxy-2,2,6-trimethyl-4-oxocyclohexyl]-3-methylpenta-2,4-dienoic acid	C[C@H]1CC(=O)CC(C1(/C=C/C(=C\C(=O)O)/C)O)(C)C	-9.46206	0.56172

Minimized affinity ≤ −10.0: very strong binding affinity; −9.0 to −10.0: strong binding affinity; −7.0 to −9.0: moderate binding affinity; *RMSD*≤ 1.0 Å: highly stable structural pose; 1.0 – 2.0 Å: acceptable stability; 2.0 – 3.0 Å: moderately stable; > 3.0 Å: unstable structural pose.

Table 7: Zmply9 Models without Ligand and Receptor Shape Restrictions

S/N	Pubchem ID	Compound Name	SMILEs	Minimized affinity (kcal/mol)	Minimized RMSD
1	121247699	(2Z,4E)-5-[(1S,4S)-1-hydroxy-2,6,6-trimethyl-4-(3-naphthalen-1-ylprop-2-ynoxy)cyclohex-2-en-1-yl]-3-methylpenta-2,4-dienoic acid	CC1=C[C@H](CC([C@]1(/C=C/C(=C\C(=O)O)/C)O)(C)C)OCC#CC2=CC=CC3=CC=CC=C32	-10.4523	2.80094
2	10313782	(2Z,4E)-5-[(1R,6S)-1-hydroxy-2,6-dimethyl-4-oxo-6-(trifluoromethyl)cyclohex-2-en-1-yl]-3-methylpenta-2,4-dienoic acid	CC1=CC(=O)C[C@]([C@]1(/C=C/C(=C\C(=O)O)/C)O)(C)C(F)(F)F	-10.071	0.92577
3	118646321	(2Z,4E)-5-[(1R)-3-[(4-chlorophenyl)methyl]-1-hydroxy-2,6,6-trimethyl-4-oxocyclohex-2-en-1-yl]-3-methylpenta-2,4-dienoic acid	CC1=C(C(=O)CC([C@@]1(/C=C/C(=C\C(=O)O)/C)O)(C)C)CC2=CC=C(C=C2)Cl	-9.91668	2.39258
4	10336004	(2Z,4E)-5-[(1R,6R)-1-hydroxy-2,6-dimethyl-4-oxo-6-(trifluoromethyl)cyclohex-2-en-1-yl]-3-methylpenta-2,4-dienoic acid	CC1=CC(=O)C[C@@]([C@]1(/C=C/C(=C\C(=O)O)/C)O)(C)C(F)(F)F	-9.90138	0.86381
5	163081310	5-(5-formyl-1,2,4a-trimethyl-2,3,4,7,8,8a-hexahydronaphthalen-1-yl)-3-methylpent-2-enoic acid	CC1CCC2(C(C1(C)CCC(=CC(=O)O)C)CCC=C2C=O)C	-9.84752	1.15593
6	15479571	(2Z,4E)-5-[(1S,6R)-3-fluoro-1-hydroxy-6-(hydroxymethyl)-2,6-dimethyl-4-oxocyclohex-2-en-1-yl]-3-methylpenta-2,4-dienoic acid	CC1=C(C(=O)C[C@]([C@]1(/C=C/C(=C\\C(=O)O)/C)O)(C)CO)F	-9.82287	0.84641
7	10379033	(2Z,4E)-5-[(1S)-3-fluoro-1-hydroxy-2,6,6-trimethyl-4-oxocyclohex-2-en-1-yl]-3-methylpenta-2,4-dienoic acid	CC1=C(C(=O)CC([C@]1(/C=C/C(=C\\C(=O)O)/C)O)(C)C)F	-9.79267	0.81345
8	10661840	(2Z,4E)-5-[(1S)-3-chloro-1-hydroxy-2,6,6-trimethyl-4-oxocyclohex-2-en-1-yl]-3-methylpenta-2,4-dienoic acid	CC1=C(C(=O)CC([C@]1(/C=C/C(=C\\C(=O)O)/C)O)(C)C)Cl	-9.72272	0.93906
9	148240468	(2Z,4Z)-5-hydroxy-5-[(1S)-1-hydroxy-2,6,6-trimethyl-4-oxocyclohex-2-en-1-yl]-3-methylpenta-2,4-dienoic acid	CC1=CC(=O)CC([C@]1(/C(=C/C(=C\\C(=O)O)/C)/O)O)(C)C	-9.5984	0.76525
10	118646136	(2Z,4E)-5-[3-(difluoromethyl)-1-hydroxy-2,6,6-trimethyl-4-oxocyclohex-2-en-1-yl]-3-methylpenta-2,4-dienoic acid	CC1=C(C(=O)CC(C1(/C=C/C(=C\\C(=O)O)/C)O)(C)C)C(F)F	-9.59762	1.02251
11	10588337	(2Z,4E)-5-[(1S)-1-hydroxy-4-oxo-2,6,6-tris(trideuteriomethyl)cyclohex-2-en-1-yl]-3-methylpenta-2,4-dienoic acid	[2H]C([2H])([2H])C1=CC(=O)CC([C@]1(/C=C/C(=C\\C(=O)O)/C)O)(C([2H])([2H])[2H])C([2H])([2H])[2H]	-9.54427	0.7284
12	101949275	(2Z,4E)-5-[(6S)-1-hydroxy-2,2,6-trimethyl-4-oxocyclohexyl]-3-methylpenta-2,4-dienoic acid	C[C@H]1CC(=O)CC(C1(/C=C/C(=C\\C(=O)O)/C)O)(C)C	-9.52701	0.67413
13	7251168	(2Z,4E)-5-[(1S)-1-hydroxy-2,6,6-trimethyl-4-oxocyclohex-2-en-1-yl]-3-methylpenta-2,4-dienoate	CC1=CC(=O)CC([C@]1(/C=C/C(=C\\C(=O)[O-])/C)O)(C)C	-9.51977	0.72359
14	100970107	(2Z,4E)-3-methyl-5-[(1S)-2,6,6-trimethyl-1-(18O)oxidanyl-4-oxocyclohex-2-en-1-yl]penta-2,4-dienoic acid	CC1=CC(=O)CC([C@]1(/C=C/C(=C\\C(=O)O)/C)[18OH])(C)C	-9.5171	0.72282
15	100970109	(2Z,4E)-5-[(1S)-1-hydroxy-2,6,6-trimethyl-4-(18O)oxocyclohex-2-en-1-yl]-3-methylpenta-2,4-dienoic acid	CC1=CC(=[18O])CC([C@]1(/C=C/C(=C\\C(=O)O)/C)O)(C)C	-9.5171	0.72282

S/N	Pubchem ID	Compound Name	SMILEs	Minimized affinity (kcal/mol)	Minimized RMSD
16	11054574	(2Z,4E)-5-deuterio-5-(1-hydroxy-2,6,6-trimethyl-4-oxocyclohex-2-en-1-yl)-3-methylpenta-2,4-dienoic acid	[2H]/C(=C\\C(=C/C(=O)O)\\C)/C1(C(=CC(=O)CC1(C)C)C)O	-9.4959	0.84075
17	44603163	(2Z,4E)-5-[(1R,6R)-6-ethynyl-1-hydroxy-2,6-dimethyl-4-oxocyclohex-2-en-1-yl]-3-methylpenta-2,4-dienoic acid	CC1=CC(=O)C[C@]([C@]1(/C=C/C(=C\\C(=O)O)/C)O)(C)C#C	-9.47773	0.79587
18	166176980	(2Z,4E)-5-[(1R,6R)-5,5-dideuterio-1-hydroxy-6-(hydroxymethyl)-6-methyl-4-oxo-2-(trideuteriomethyl)cyclohex-2-en-1-yl]-3-(trideuteriomethyl)penta-2,4-dienoic acid	[2H]C1(C(=O)C=C([C@@]([C@@]1(C)CO)(/C=C/C(=C\\C(=O)O)/C([2H])([2H])[2H])O)C([2H])([2H])[2H])[2H]	-9.45733	0.69664
19	10849377	(2Z,4E)-5-[(1S)-1-fluoro-2,6,6-trimethyl-4-oxocyclohex-2-en-1-yl]-3-methylpenta-2,4-dienoic acid	CC1=CC(=O)CC([C@]1(/C=C/C(=C\\C(=O)O)/C)F)(C)C	-9.42205	0.54949
20	87059898	(2Z)-5-(1-hydroxy-2,6,6-trimethyl-4-oxocyclohex-2-en-1-yl)-3-methylpenta-2,4-dienoic acid	CC1=CC(=O)CC(C1(C=C/C(=C\\C(=O)O)/C)O)(C)C	-9.41995	0.60325
21	13629014	(2Z,4E)-5-[(1S,4S)-1,4-dihydroxy-2,6,6-trimethylcyclohex-2-en-1-yl]-3-methylpenta-2,4-dienoic acid	CC1=C[C@H](CC([C@]1(/C=C/C(=C\\C(=O)O)/C)O)(C)C)O	-9.41751	0.62104
22	102303458	(2Z,4E)-5-[(1S)-1-hydroxy-2-methyl-4-oxo-6,6-bis(trideuteriomethyl)cyclohex-2-en-1-yl]-3-methylpenta-2,4-dienoic acid	[2H]C([2H])([2H])C1(CC(=O)C=C([C@@]1(/C=C/C(=C\\C(=O)O)/C)O)C)C([2H])([2H])[2H]	-9.39084	0.66024
23	163817160	(2Z,4E)-5-[(1S)-1-hydroxy-2,6,6-trimethyl-4-oxocyclohex-2-en-1-yl]-3,4-dimethylpenta-2,4-dienoic acid	CC1=CC(=O)CC([C@]1(/C=C(\\C)/C(=C\\C(=O)O)/C)O)(C)C	-9.36431	1.13976
24	102094723	(2Z,4E)-5-[(1R,6R)-6-ethenyl-1-hydroxy-2,6-dimethyl-4-oxocyclohex-2-en-1-yl]-3-methylpenta-2,4-dienoic acid	CC1=CC(=O)C[C@]([C@]1(/C=C/C(=C\\C(=O)O)/C)O)(C)C=C	-9.35344	0.71277
25	126628112	(2Z,4E)-5-[(1R,6R)-6-cyclopropyl-1-hydroxy-2,6-dimethyl-4-oxocyclohex-2-en-1-yl]-3-methylpenta-2,4-dienoic acid	CC1=CC(=O)C[C@]([C@]1(/C=C/C(=C\\C(=O)O)/C)O)(C)C2CC2	-9.34707	0.68751
26	141813086	(2Z,4E)-3-methyl-5-(2,2,6-trimethyl-4-oxocyclohexyl)penta-2,4-dienoic acid	CC1CC(=O)CC(C1/C=C/C(=C\\C(=O)O)/C)(C)C	-9.33654	0.65848
27	141813054	(2Z,4E)-5-[(1S,6S)-2-cyano-1-hydroxy-2,6-dimethyl-4-oxocyclohexyl]-3-methylpenta-2,4-dienoic acid	C[C@H]1CC(=O)CC([C@]1(/C=C/C(=C\\C(=O)O)/C)O)(C)C#N	-9.33266	0.6399
28	10514699	(2Z,4E)-3-methyl-5-[(1R)-2,6,6-trimethyl-4-oxocyclohex-2-en-1-yl]penta-2,4-dienoic acid	CC1=CC(=O)CC([C@H]1/C=C/C(=C\\C(=O)O)/C)(C)C	-9.31502	0.74718
29	50909797	(2Z,4E)-3-methyl-5-(2,6,6-trimethyl-4-oxocyclohex-2-en-1-yl)penta-2,4-dienoic acid	CC1=CC(=O)CC(C1/C=C/C(=C\\C(=O)O)/C)(C)C	-9.30668	0.73461
30	129320420	(2Z,4E)-3-methyl-5-[(1R)-2,6,6-trimethyl-4-oxocyclohex-2-en-1-yl]penta-2,4-dienoate	CC1=CC(=O)CC([C@H]1/C=C/C(=C\\C(=O)[O-])/C)(C)C	-9.30373	0.73451
31	134553060	(2Z,4E)-5-[(1R)-1-hydroxy-2,6,6-trimethyl-4-oxocyclohex-2-en-1-yl]-3-methylhexa-2,4-dienoic acid	CC1=CC(=O)CC([C@]1(/C(=C/C(=C\\C(=O)O)/C)/C)O)(C)C	-9.30012	0.77598
32	121247701	(2Z,4E)-5-[(1S,4S)-1-hydroxy-2,6,6-trimethyl-4-[3-(4-methylphenyl)prop-2-ynoxy]cyclohex-2-en-1-yl]-3-methylpenta-2,4-dienoic acid	CC1=CC=C(C=C1)C#CCO[C@H]2CC([C@](C(=C2)C)(/C=C/C(=C\\C(=O)O)/C)O)(C)C	-9.28344	2.85051
33	101222923	(2Z,4E)-5-[(1S,4S)-1-hydroxy-2,6,6-trimethyl-4-phenylmethoxycyclohex-2-en-1-yl]-3-methylpenta-2,4-dienoic acid	CC1=C[C@H](CC([C@]1(/C=C/C(=C\\C(=O)O)/C)O)(C)C)OCC2=CC=CC=C2	-9.27178	1.81567
34	101949279	(Z)-5-[(6S)-1-hydroxy-2,2,6-trimethyl-4-oxocyclohexyl]-3-methylpent-2-en-4-ynoic acid	C[C@H]1CC(=O)CC(C1(C#C/C(=C\\C(=O)O)/C)O)(C)C	-9.26966	0.65332
35	118646590	(2Z,4E)-5-[(1R)-3-[(3,4-difluorophenyl)methyl]-1-hydroxy-2,6,6-trimethyl-4-oxocyclohex-2-en-1-yl]-3-methylpenta-2,4-dienoic acid	CC1=C(C(=O)CC([C@@]1(/C=C/C(=C\\C(=O)O)/C)O)(C)C)CC2=CC(=C(C=C2)F)F	-9.24567	2.46274

S/N	Pubchem ID	Compound Name	SMILEs	Minimized affinity (kcal/mol)	Minimized RMSD
36	14702799	(2Z,4E)-5-[(1R,6R)-1-hydroxy-2,2,6-trimethyl-4-oxocyclohexyl]-3-methylpenta-2,4-dienoic acid	C[C@@H]1CC(=O)CC([C@@]1(/C=C/C(=C\\C(=O)O)/C)O)(C)C	-9.24176	1.1677
37	89052205	(2Z,4E)-5-(6-ethynyl-1-hydroxy-2,6-dimethyl-4-oxocyclohex-2-en-1-yl)-3-methylpenta-2,4-dienoic acid	CC1=CC(=O)CC(C1(/C=C/C(=C\\C(=O)O)/C)O)(C)C#C	-9.19971	1.26394
38	118646353	(2Z,4E)-5-[(1S)-3-ethyl-1-hydroxy-2,6,6-trimethyl-4-oxocyclohex-2-en-1-yl]-3-methylpenta-2,4-dienoic acid	CCC1=C([C@@](C(CC1=O)(C)C)(/C=C/C(=C\\C(=O)O)/C)O)C	-9.19667	1.02991
39	10563698	(2Z,4E)-5-[(1R)-1-fluoro-2,6,6-trimethyl-4-oxocyclohex-2-en-1-yl]-3-methylpenta-2,4-dienoic acid	CC1=CC(=O)CC([C@@]1(/C=C/C(=C\\C(=O)O)/C)F)(C)C	-9.1888	1.26995
40	151545313	(2Z,4E)-5-[(1S)-1-hydroxy-2,6,6-trimethyl-4-oxo-3-phenylcyclohex-2-en-1-yl]-3-methylpenta-2,4-dienoic acid	CC1=C(C(=O)CC([C@]1(/C=C/C(=C\\C(=O)O)/C)O)(C)C)C2=CC=CC=C2	-9.17337	3.16646
41	118225409	(2Z,4E)-5-(5-hydroxy-2,3,6,6-tetramethyl-4-oxocyclohex-2-en-1-yl)-3-methylpenta-2,4-dienoic acid	CC1=C(C(=O)C(C(C1/C=C/C(=C\\C(=O)O)/C)(C)C)O)C	-9.13328	0.9173

Minimized affinity ≤ −10.0: very strong binding affinity; −9.0 to −10.0: strong binding affinity; −7.0 to −9.0: moderate binding affinity; *RMSD*≤ 1.0 Å: highly stable structural pose; 1.0 – 2.0 Å: acceptable stability; 2.0 – 3.0 Å: moderately stable; > 3.0 Å: unstable structural pose.

Table 8: Zmply12 Models without Ligand and Receptor Shape Restrictions

S/N	Pubchem ID	Compound Name	SMILEs	Minimized affinity (kcal/mol)	Minimized RMSD
1	10084402	2-[(2R,4aR,8R,8aR)-8,8a-dihydroxy-4a,8-dimethyl-2,3,4,5,6,7-hexahydro-1H-naphthalen-2-yl]prop-2-enoic acid	C[C@]12CCC[C@@]([C@]1(C[C@@H](CC2)C(=C)C(=O)O)O)(C)O	-9.79227	0.90384
2	90074494	(2Z,4E)-3-cyclopropyl-5-[1-hydroxy-2,6-dimethyl-4-oxo-6-(trifluoromethyl)cyclohex-2-en-1-yl]penta-2,4-dienoic acid	CC1=CC(=O)CC(C1(/C=C/C(=C\\C(=O)O)/C2CC2)O)(C)C(F)(F)F	-9.26572	0.80349
3	10336005	(2Z,4E)-5-[(1S,6R)-1-hydroxy-2,6-dimethyl-4-oxo-6-(trifluoromethyl)cyclohex-2-en-1-yl]-3-methylpenta-2,4-dienoic acid	CC1=CC(=O)C[C@@]([C@@]1(/C=C/C(=C\\C(=O)O)/C)O)(C)C(F)(F)F	-9.12092	1.67296
4	10563417	(2Z,4E)-5-[(1R,2S,6S)-2-hydroxy-1,3-dimethyl-5-oxo-2-bicyclo[4.1.0]hept-3-enyl]-3-methylpenta-2,4-dienoic acid	CC1=CC(=O)[C@H]2C[C@]2([C@@]1(/C=C/C(=C\\C(=O)O)/C)O)C	-9.09305	1.13081
5	162860100	2-(8,8a-dihydroxy-4a,8-dimethyl-2,3,4,5,6,7-hexahydro-1H-naphthalen-2-yl)prop-2-enoic acid	CC12CCCC(C1(CC(CC2)C(=C)C(=O)O)O)(C)O	-9.05648	1.10683
6	10753936	(2Z,4E)-5-[(1R,2R,6S)-2-hydroxy-1,3-dimethyl-5-oxo-2-bicyclo[4.1.0]hept-3-enyl]-3-methylpenta-2,4-dienoic acid	CC1=CC(=O)[C@H]2C[C@]2([C@]1(/C=C/C(=C\\C(=O)O)/C)O)C	-9.00559	1.02548
7	134611692	(2Z,4E)-3-cyclopropyl-5-[(1S)-1-hydroxy-2,6,6-trimethyl-4-oxocyclohex-2-en-1-yl]penta-2,4-dienoic acid	CC1=CC(=O)CC([C@]1(/C=C/C(=C\\C(=O)O)/C2CC2)O)(C)C	-8.99014	0.72415
8	158950221	(2Z,4E)-4,5-dideuterio-5-[(1S)-2-(deuteriomethyl)-1-hydroxy-6,6-dimethyl-4-oxocyclohex-2-en-1-yl]-3-(trideuteriomethyl)penta-2,4-dienoic acid	[2H]CC1=CC(=O)CC([C@]1(/C(=C(\\[2H])/C(=C\\C(=O)O)/C([2H])([2H])[2H])/[2H])O)(C)C	-8.96669	0.83465
9	89971570	(Z)-5-(2-hydroxy-1,3-dimethyl-5-oxo-2-bicyclo[4.1.0]hept-3-enyl)-3-methylpent-2-en-4-ynoic acid	CC1=CC(=O)C2CC2(C1(C#C/C(=C\\C(=O)O)/C)O)C	-8.96622	1.10489
10	10086154	(2Z,4E)-5-[(1S,6S)-6-(difluoromethyl)-1-hydroxy-2,6-dimethyl-4-oxocyclohex-2-en-1-yl]-3-methylpenta-2,4-dienoic acid	CC1=CC(=O)C[C@]([C@@]1(/C=C/C(=C\\C(=O)O)/C)O)(C)C(F)F	-8.90608	1.23231
11	89095877	(2Z,4E)-3-cyclopropyl-5-(2-hydroxy-1,3-dimethyl-5-oxo-2-bicyclo[4.1.0]hept-3-enyl)penta-2,4-dienoic acid	CC1=CC(=O)C2CC2(C1(/C=C/C(=C\\C(=O)O)/C3CC3)O)C	-8.78544	0.74484
12	123956510	3-cyclopropyl-5-(2-hydroxy-1,3-dimethyl-5-oxo-2-bicyclo[4.1.0]hept-3-enyl)penta-2,4-dienoic acid	CC1=CC(=O)C2CC2(C1(C=CC(=CC(=O)O)C3CC3)O)C	-8.73409	0.74213

S/N	Pubchem ID	Compound Name	SMILEs	Minimized affinity (kcal/mol)	Minimized RMSD
13	86713144	(E)-5-(1-hydroxy-2,6,6-trimethyl-4-oxocyclohex-2-en-1-yl)-3-(trifluoromethyl)pent-2-en-4-ynoic acid	CC1=CC(=O)CC(C1(C#C/C(=C\\C(=O)O)/C(F)(F)F)O)(C)C	-8.72314	1.69577
14	7054951	(3R)-5-[(1R,2R,4aR,8aR)-2-hydroxy-2,5,5,8a-tetramethyl-3,4,4a,6,7,8-hexahydro-1H-naphthalen-1-yl]-3-methylpentanoic acid	C[C@H](CC[C@@H]1[C@@]2(CCCC([C@H]2CC[C@@]1(C)O)(C)C)C)CC(=O)O	-8.69235	1.75514
15	89052380			-8.68376	2.70385
16	10731592	(2Z,4E)-5-[(1S,6R)-6-(fluoromethyl)-1-hydroxy-2,6-dimethyl-4-oxocyclohex-2-en-1-yl]-3-methylpenta-2,4-dienoic acid	CC1=CC(=O)C[C@@]([C@@]1(/C=C/C(=C\\C(=O)O)/C)O)(C)CF	-8.67757	1.67909
17	67652154	2-acetyl-4-[(8'S,9'S,10'R,13'S,14'S,17'S)-17'-hydroxy-13'-methyl-11'-methylidenespiro[1,3-dioxolane-2,3'-2,4,7,8,9,10,12,14,15,16-decahydro-1H-cyclopenta[a]phenanthrene]-17'-yl]pent-4-enoic acid	CC(=O)C(CC(=C)[C@]1(CC[C@@H]2[C@@]1(CC(=C)[C@H]3[C@H]2CC=C4[C@@H]3CCC5(C4)OCCO5)C)O)C(=O)O	-8.66153	3.14042
18	126616051	(2Z,4E)-5-(6-cyclopropyl-1-hydroxy-2,6-dimethyl-4-oxocyclohex-2-en-1-yl)-3-methylpenta-2,4-dienoic acid	CC1=CC(=O)CC(C1(/C=C/C(=C\\C(=O)O)/C)O)(C)C2CC2	-8.64424	1.56486
19	131841575	(2Z,4E)-5-[(1S,4S)-1,4-dihydroxy-2,2-dimethyl-6-methylidenecyclohexyl]-3-methylpenta-2,4-dienoate	C/C(=C/C(=O)[O-])/C=C/[C@]1(C(=C)C[C@H](CC1(C)C)O)O	-8.48278	0.72778
20	118721173	(2Z,4E)-5-(1,4-dihydroxy-2,6,6-trimethylcyclohex-2-en-1-yl)-3-methylpenta-2,4-dienoic acid	CC1=CC(CC(C1(/C=C/C(=C\\C(=O)O)/C)O)(C)C)O	-8.47115	1.34716
21	52921581	(2Z,4E)-5-[(1R,5R,8S)-8-hydroxy-1,5-dimethyl-3-oxo-6-oxabicyclo[3.2.1]octan-8-yl]-3-methylpenta-2,4-dienoate	C/C(=C/C(=O)[O-])/C=C/[C@@]1([C@@]2(CC(=O)C[C@]1(OC2)C)C)O	-8.4526	1.1243
22	73152384	5-[1-hydroxy-6-(hydroxymethyl)-2,6-dimethyl-4-oxocyclohex-2-en-1-yl]-3-methylpenta-2,4-dienoic acid	CC1=CC(=O)CC(C1(C=CC(=CC(=O)O)C)O)(C)CO	-8.43126	1.70895
23	70386599	(Z)-5-[(1S,2R,4aR,8aR)-2-hydroxy-2,5,5,8a-tetramethyl-3,4,4a,6,7,8-hexahydro-1H-naphthalen-1-yl]-3-methylpent-2-enoic acid	C/C(=C/C(=O)O)/CC[C@H]1[C@@]2(CCCC([C@H]2CC[C@@]1(C)O)(C)C)C	-8.12432	1.64359
24	83043377	2-[1-hydroxy-1-(2,4,6-trimethylphenyl)ethyl]pentanoic acid	CCCC(C(=O)O)C(C)(C1=C(C=C(C=C1C)C)C)O	-8.07685	1.66084
24	114392524	2-[hydroxy-(2,4,6-trimethylphenyl)methyl]-4-methylcyclopentane-1-carboxylic acid	CC1CC(C(C1)C(=O)O)C(C2=C(C=C(C=C2C)C)C)O	-8.03801	0.97984
26	74763347	(Z)-3-[2-(1-hydroxy-2,2,6-trimethylcyclohexyl)ethynyl]hex-2-enoic acid	CCC/C(=C/C(=O)O)/C#CC1(C(CCCC1(C)C)C)O	-8.02397	0.90453
27	104233182	2-[1-(2-fluoro-6-methoxyphenyl)-1-hydroxyethyl]hexanoic acid	CCCCC(C(=O)O)C(C)(C1=C(C=CC=C1F)OC)O	-7.992	1.19751
28	80047440	2-[1-hydroxy-1-(2,4,6-trimethylphenyl)ethyl]hexanoic acid	CCCCC(C(=O)O)C(C)(C1=C(C=C(C=C1C)C)C)O	-7.98695	1.93853
29	162681575	tetrasodium;tetrakis(1,4,5,6-tetrafluoro-5-fluorooxy-3,4-dihydroxy-6-phenylcyclohex-2-ene-1-carboxylate)	C1=CC=C(C=C1)C2(C(C=C(C(C2(OF)F)(O)F)O)(C(=O)[O-])F)F.C1=CC=C(C=C1)C2(C(C=C(C(C2(OF)F)(O)F)O)(C(=O)[O-])F)F.C1=CC=C(C=C1)C2(C(C=C(C(C2(OF)F)(O)F)O)(C(=O)[O-])F)F.C1=CC=C(C=C1)C2(C(C=C(C(C2(OF)F)(O)F)O)(C(=O)[O-])F)F.[Na+].[Na+].[Na+].[Na+]	-7.89236	0.99734
30	83042765	2-[hydroxy-(2,4,6-trimethylphenyl)methyl]pentanoic acid	CCCC(C(C1=C(C=C(C=C1C)C)C)O)C(=O)O	-7.60666	1.50613
31	23243281	2-[(2R,4aS,7R,8R,8aR)-7-acetyloxy-8-hydroxy-4a,8-dimethyl-1,2,3,4,5,6,7,8a-octahydronaphthalen-2-yl]prop-2-enoic acid	CC(=O)O[C@@H]1CC[C@@]2(CC[C@H](C[C@H]2[C@@]1(C)O)C(=C)C(=O)O)C	-7.56858	0.96195
32	83042450	2-[1-(2,6-difluorophenyl)-1-hydroxyethyl]pentanoic acid	CCCC(C(=O)O)C(C)(C1=C(C=CC=C1F)F)O	-7.53388	1.17583

S/N	Pubchem ID	Compound Name	SMILEs	Minimized affinity (kcal/mol)	Minimized RMSD
33	90074298	(E)-5-[(4Z)-1-hydroxy-4-methoxyimino-2,6,6-trimethylcyclohex-2-en-1-yl]-3-(trifluoromethyl)pent-2-en-4-ynoic acid	CC1=C/C(=N\\OC)/CC(C1(C#C/C(=C\\C(=O)O)/C(F)(F)F)O)(C)C	-7.48516	1.13565
34	54559505	2,2-bis(2,6-diethyl-2,3,6-trimethylpiperidin-4-yl)propanedioic acid	CCC1(CC(C(C(N1)(C)CC)C)C(C2CC(NC(C2C)(C)CC)(C)CC)(C(=O)O)C(=O)O)C	-7.23754	1.64642
35	90039860	1-[(2R)-2-ethyl-1,2-dihydroxy-3,3-dimethylpentyl]pyrrolidine-2-carboxylic acid	CC[C@](C(N1CCCC1C(=O)O)O)(C(C)(C)CC)O	-7.22726	3.6955
36	82348902	3-(tert-butylamino)-4-hydroxy-4-(2,4,6-trimethylphenyl)butanoic acid	CC1=CC(=C(C(=C1)C)C(C(CC(=O)O)NC(C)(C)C)O)C	-7.14046	1.79303
37	148243429			-7.11292	1.42657
38	141244025	3-[[5-[(4-acetyl-3-hydroxy-2-methylphenoxy)methyl]-1H-pyrazol-3-yl]methyl]benzoic acid	CC1=C(C=CC(=C1O)C(=O)C)OCC2=CC(=NN2)CC3=CC(=CC=C3)C(=O)O	-7.07376	3.7007
39	60199733	(E)-4-[(1R,3R,6R,7S,8R)-1,7-dihydroxy-3,6-dimethyl-4-oxatricyclo[4.2.1.03,7]nonan-8-yl]-3-methylbut-3-enoic acid	C/C(=C\\[C@@H]1[C@]2(C[C@]3([C@@]1([C@@](C2)(OC3)C)O)C)O)/CC(=O)O	-7.03607	3.04926
40	162816737	2-(4,5-dihydroxy-6-methoxy-3,6-dimethyl-2-oxocyclohex-3-en-1-yl)oxy-4-hydroxy-3,6-dimethylbenzoic acid	CC1=CC(=C(C(=C1C(=O)O)OC2C(=O)C(=C(C(C2(C)OC)O)O)C)C)O	-7.02709	0.64844

Minimized affinity ≤ −10.0: very strong binding affinity; −9.0 to −10.0: strong binding affinity; −7.0 to −9.0: moderate binding affinity; *RMSD*≤ 1.0 Å: highly stable structural pose; 1.0 – 2.0 Å: acceptable stability; 2.0 – 3.0 Å: moderately stable; > 3.0 Å: unstable structural pose.

Drug-Likeness and Agrochemical Suitability

Evaluation based on Tice agrochemical rules demonstrated that nearly all compounds satisfied key criteria (MW ≤ 500 Da, HBD ≤ 3, HBA ≤ 10, LogP ≤ 5) (Tables 9 and 10) suggestive of favourable physicochemical properties for plant-targeted applications. Importantly, top-performing compounds identified through integrated screening, including 10661840, 10588337, and 134611692, fully complied with these criteria, reinforcing their suitability as agrochemical candidates. Only two compounds violated hydrogen bond donor limits (Table 11) which is indicative of a minimal deviation from optimal profiles. Overall, the ligand set exhibited a balanced hydrophilic-lipophilic profile, which is critical for plant uptake, systemic translocation, and bioavailability (Tice, 2001; Driver et al., 2020). These findings underscore the potential of the identified ABA analogues as effective plant growth regulators for stress mitigation.

Table 9: Grochemical Likeness Properties for Generated Zmply9 Ligands with Constraints

Ligands	MWT	LogP	No. Of Rotable Bonds	H-Bonds Acceptor	H-Bond Donor	TPSA	Rule of 5 violations
14702801	266.33	2.06	3	4	2	74.6	0
14702801	266.33	2.08	3	4	2	74.6	0
141780114	266.33	2.02	3	4	2	74.6	0
141812992	266.33	2.02	3	4	2	74.6	0

Table 10: Agrochemical Likeness Properties for Generated Zmply9 Ligands without Constraints

Ligands	MWT	LogP	No. Of Rotable Bonds	H-Bonds Acceptor	H-Bond Donor	TPSA	Rule of 5 violations
118646321	388.88	4.07	5	4	2	74.6	0
10336004	318.29	4.07	4	7	2	74.6	0
163081310	318.45	4.19	5	3	1	54.37	0
15479571	298.31	1.64	4	6	3	94.83	0
10379033	282.31	1.64	3	5	2	74.6	0
10661840	298.76	1.64	3	4	2	74.6	0
148240468	280.32	1.64	3	5	3	94.83	0
118646136	314.32	1.64	4	6	2	74.6	0
10588337	273.37	1.64	3	4	2	74.6	0
101949275	266.33	2.02	3	4	2	74.6	0
44603163	274.31	1.93	3	4	2	74.6	0
166176980	288.37	1.24	4	5	3	94.83	0
10849377	266.31	1.24	3	4	1	54.37	0
87059898	264.32	1.96	3	4	2	74.6	0
13629014	266.33	1.96	3	4	3	77.76	0
102303458	270.35	1.96	3	4	2	74.6	0
102094723	276.33	2.2	4	4	2	2.2	0
126628112	290.35	2.2	4	4	2	2.2	0

Ligands	MWT	LogP	No. Of Rotable Bonds	H-Bonds Acceptor	H-Bond Donor	TPSA	Rule of 5 violations
141813086	250.33	2.66	3	3	1	2.66	0
141813054	277.32	1.45	3	5	2	1.45	0
10514699	248.32	1.45	3	3	1	1.45	0
50909797	248.32	1.45	3	3	1	1.45	0
129320420	247.31	1.45	3	3	0	1.45	0
134553060	278.34	1.45	3	4	2	1.45	0
121247701	394.5	1.45	5	4	2	1.45	0
101949279	264.32	1.92	1	4	2	74.6	0
118646590	390.42	1.92	5	6	2	74.6	0
14702799	266.33	2.1	3	4	2	74.6	0
89052205	274.31	1.93	3	4	2	74.6	0
118646353	292.37	2.65	4	4	2	74.6	0
10563698	266.31	2.65	3	4	1	54.37	0
151545313	340.41	2.65	4	4	2	74.6	0
118225409	278.34	2.65	3	4	2	74.6	0

Compounds highlighted in red violated at least 1 rule of the agrochemical-likeness properties

Table 11: Agrochemical Likeness Properties for Generated Zmply12 Ligands without Constraints

Ligands	MWT	LogP	No. Of Rotable Bonds	H-Bonds Acceptor	H-Bond Donor	TPSA	Rule of 5 violations
162860100	268.35	1.95	2	4	3	77.76	0
10753936	262.3	1.95	3	4	2	74.6	0
134611692	290.35	1.95	4	4	2	74.6	0
158950221	270.35	1.95	3	4	2	74.6	0
89971570	260.29	1.58	1	4	2	74.6	0
10086154	300.3	1.58	4	6	2	74.6	0
89095877	288.34	1.58	4	4	2	74.6	0
123956510	288.34	2.17	4	4	2	74.6	0
86713144	316.27	2.46	2	7	2	74.6	0
7054951	324.5	4.28	5	3	2	57.53	0
10731592	282.31	2.07	4	5	2	74.6	0
67652154	470.6	3.66	5	6	2	93.06	0
126616051	290.35	3.66	4	4	2	74.6	0
131841575	265.32	1.72	3	4	2	80.59	0
118721173	266.33	1.72	3	4	3	77.76	0
52921581	279.31	1.72	3	5	1	86.66	0
73152384	280.32	1.3	4	5	3	94.83	0
70386599	322.48	4.26	4	3	2	57.53	0
83043377	264.36	3.11	5	3	2	57.53	0
114392524	276.37	3.08	3	3	2	57.53	0
74763347	278.39	3.42	3	3	2	57.53	0
104233182	284.32	2.81	7	5	2	66.76	0
80047440	278.39	3.59	6	3	2	57.53	0
83042765	250.33	3	5	3	2	57.53	0
23243281	310.39	2.34	4	5	2	83.83	0
83042450	258.26	2.85	5	5	2	57.53	0
90074298	345.31	2.85	3	8	2	79.12	0
54559505	466.7	3.46	8	6	4	98.66	1
90039860	273.37	0.97	6	5	3	81	0
82348902	293.4	2.17	6	4	3	69.56	0
141244025	380.39	2.98	7	6	3	112.51	0
60199733	282.33	1.2	3	5	3	86.99	0
162816737	366.36	1.13	4	8	4	133.52	1
10084402	268.35	2.01	2	4	3	77.76	0
90074494	344.33	2.01	5	7	2	74.6	0
10336005	318.29	2.01	4	7	2	74.6	0
10563417	262.3	2.01	3	4	2	74.6	0

Compounds highlighted in red violated at least 1 rule of the agrochemical-likeness properties

ADMET and Pharmacokinetic Properties

ADMET analysis revealed highly favourable pharmacokinetic properties across the ligand library. All top-ranked compounds, including 10661840, 10588337, 10379033, and 134611692, exhibited high gastrointestinal absorption, suggesting efficient uptake and systemic distribution (). Most compounds were predicted to be non-substrates of P-glycoprotein, indicating reduced efflux and enhanced intracellular retention. Importantly, minimal inhibition of major cytochrome P450 enzymes (CYP1A2, CYP2C9, CYP2D6, and CYP3A4) was observed among the leading compounds, suggesting low metabolic interference and reduced likelihood of off-target toxicity. Although moderate blood-brain barrier permeability was predicted for some ligands, this property is of limited relevance in plant systems. Collectively, these pharmacokinetic profiles indicate strong bioavailability, metabolic stability, and environmental compatibility, which are essential attributes for agrochemical development (Daina et al., 2017; Pires et al., 2015).

Table 12: Pharmacokinetic Properties of Generated Ligands for Zmply9 with Constraints

Pubchem ID	GI Absorption	BBB	P-gp Substrate	CYP1A2 inhibitor	CYP2C19 inhibitor	CYP2C9 inhibitor	CYP2D6 inhibitor	CYP3A4 inhibitor	Log K_p (skin permeation)
14702801	High	Yes	No	No	No	No	No	No	-6.56
14702801	High	Yes	No	No	No	No	No	No	-6.56
141780114	High	Yes	No	No	No	No	No	No	-6.56
141812992	High	Yes	No	No	No	No	No	No	-6.56

Table 13: Pharmacokinetic Properties of Generated Ligands for Zmply9 without Constraints

Pubchem ID	GI Absorption	BBB	P-gp Substrate	CYP1A2 inhibitor	CYP2C19 inhibitor	CYP2C9 inhibitor	CYP2D6 inhibitor	CYP3A4 inhibitor	Log K_p (skin permeation)
118646321	High	No	No	No	Yes	Yes	No	Yes	-5.71
10336004	High	No	No	No	Yes	Yes	No	Yes	-5.71
163081310	High	Yes	No	No	Yes	Yes	No	Yes	-4.37
15479571	High	No	No	No	No	No	No	No	-7.23
10379033	High	No	No	No	No	No	No	No	-7.23
10661840	High	No	No	No	No	No	No	No	-7.23
148240468	High	No	No	No	No	No	No	No	-7.23
118646136	High	No	No	No	No	No	No	No	-7.23
10588337	High	No	No	No	No	No	No	No	-7.23
101949275	High	Yes	No	No	No	No	No	No	-6.56
44603163	High	Yes	No	No	No	No	No	No	-7.03
166176980	High	No	No	No	No	No	No	No	-7.39
10849377	High	No	No	No	No	No	No	No	-7.39
87059898	High	Yes	No	No	No	No	No	No	-6.77
13629014	High	Yes	No	No	No	No	No	No	-6.77
102303458	High	Yes	No	No	No	No	No	No	-6.77
102094723	High	Yes	No	No	No	No	No	No	-6.66
126628112	High	Yes	No	No	No	No	No	No	-6.66
141813086	High	Yes	No	No	No	No	No	No	-5.7
141813054	High	No	No	No	No	No	No	No	-7.02
10514699	High	No	No	No	No	No	No	No	-7.02
50909797	High	No	No	No	No	No	No	No	-7.02
129320420	High	No	No	No	No	No	No	No	-7.02
134553060	High	No	No	No	No	No	No	No	-7.02
121247701	High	No	No	No	No	No	No	No	-7.02
101949279	High	Yes	No	No	No	No	No	No	-6.73
118646590	High	Yes	No	No	No	No	No	No	-6.73
14702799	High	Yes	No	No	No	No	No	No	-6.56
89052205	High	Yes	No	No	No	No	No	No	-7.03
118646353	High	Yes	No	No	Yes	No	No	No	-6.37
10563698	High	Yes	No	No	Yes	No	No	No	-6.37
151545313	High	Yes	No	No	Yes	No	No	No	-6.37
118225409	High	Yes	No	No	Yes	No	No	No	-6.37

Compounds highlighted in red had at least 2 violations

Table 14: Pharmacokinetic Properties of Generated Ligands for Zmply12 without Constraints

Pubchem ID	GI Absorption	BBB	P-gp Substrate	CYP1A2 inhibitor	CYP2C19 inhibitor	CYP2C9 inhibitor	CYP2D6 inhibitor	CYP3A4 inhibitor	Log K_p (skin permeation)
162860100	High	No	No	No	No	No	No	No	-6.7
10753936	High	No	No	No	No	No	No	No	-6.7
134611692	High	No	No	No	No	No	No	No	-6.7
158950221	High	No	No	No	No	No	No	No	-6.7
89971570	High	No	No	No	No	No	No	No	-7.18
10086154	High	No	No	No	No	No	No	No	-7.18
89095877	High	No	No	No	No	No	No	No	-7.18
123956510	High	Yes	No	No	No	No	No	No	-6.8
86713144	High	Yes	No	No	No	No	No	No	-6.89
7054951	High	Yes	No	No	No	Yes	Yes	No	-4.57
10731592	High	Yes	No	No	No	No	No	No	-7.01
67652154	High	No	Yes	No	No	No	No	Yes	-7.09
126616051	High	No	Yes	No	No	No	No	Yes	-7.09
131841575	High	No	No	No	No	No	No	No	-6.58
118721173	High	No	No	No	No	No	No	No	-6.58
52921581	High	No	No	No	No	No	No	No	-6.58
73152384	High	No	No	No	No	No	No	No	-7.34
70386599	High	Yes	No	No	No	Yes	No	No	-4.5
83043377	High	Yes	Yes	No	No	No	No	No	-5.56
114392524	High	Yes	No	No	No	No	Yes	No	-5.69
74763347	High	Yes	No	No	No	Yes	No	No	-5
104233182	High	Yes	Yes	No	No	No	No	No	-6.02
80047440	High	Yes	Yes	No	No	No	Yes	No	-5.26
83042765	High	Yes	Yes	No	No	No	No	No	-5.6
23243281	High	No	No	No	No	No	No	No	-6.36
83042450	High	Yes	No	No	No	No	No	No	-6.15
90074298	High	Yes	No	No	No	No	No	No	-6.15
90039860	High	No	Yes	No	No	No	No	No	-8.14
82348902	High	Yes	Yes	No	No	No	Yes	No	-8.09
141244025	High	No	No	No	No	Yes	No	No	-6.18
60199733	High	No	Yes	No	No	No	No	No	-7.83
10084402	High	No	No	No	No	No	No	No	-6.7
90074494	High	No	No	No	No	No	No	No	-6.7
10336005	High	No	No	No	No	No	No	No	-6.7
10563417	High	No	No	No	No	No	No	No	-6.7

Compounds highlighted in red had at least 2 violations

Toxicity Profile

Toxicological evaluation demonstrated that the majority of compounds are non-carcinogenic, non-mutagenic, non-cytotoxic, and largely non-immunotoxic. Leading candidates such as 10661840, 10588337, and 134611692 exhibited high LD_{50} values (up to 5000 mg/kg), indicating low acute toxicity and a favourable safety margin (Table 15). Although a small subset of compounds showed minor immunotoxicity or ecotoxicity signals, these were not associated with the top-performing candidates and therefore do not significantly impact the overall safety assessment. These results support the suitability of the prioritized compounds for agricultural applications with minimal environmental risk (Banerjee et al., 2018; Petrović & Leskovac, 2026).

Table 15: Toxicity Profile

Pubchem ID	LD50 (mg/kg)	Carcinogenicity	Immunotoxicity	Mutagenicity	Cytotoxicity	BBB-Barrier	Ecotoxicity
ZmPLY9							
15479571	900	Inactive	Inactive	Inactive	Inactive	Active	Inactive
10379033	900	Inactive	Inactive	Inactive	Inactive	Active	Inactive
10661840	5000	Inactive	Inactive	Inactive	Inactive	Active	Inactive
148240468	5000	Inactive	Inactive	Inactive	Inactive	Active	Inactive
118646136	900	Inactive	Inactive	Inactive	Inactive	Active	Inactive
10588337	5000	Inactive	Inactive	Inactive	Inactive	Active	Inactive
166176980	5000	Inactive	Inactive	Inactive	Inactive	Active	Inactive
10849377	4800	Inactive	Inactive	Inactive	Inactive	Active	Active
141813054	4000	Inactive	Inactive	Inactive	Inactive	Active	Inactive
10514699	4800	Inactive	Inactive	Inactive	Inactive	Active	Inactive

Pubchem ID	LD50 (mg/kg)	Carcinogenicity	Immunotoxicity	Mutagenicity	Cytotoxicity	BBB-Barrier	Ecotoxicity
50909797	4800	Inactive	Inactive	Inactive	Inactive	Active	Inactive
129320420	4800	Inactive	Inactive	Inactive	Inactive	Active	Active
134553060	5000	Inactive	Inactive	Inactive	Inactive	Active	Inactive
121247701	4900	Inactive	Active	Inactive	Inactive	Active	Inactive
ZmPLY12							
162860100	2500	Inactive	Inactive	Inactive	Inactive	Active	Inactive
10753936	900	Inactive	Inactive	Inactive	Inactive	Active	Inactive
134611692	5000	Inactive	Inactive	Inactive	Inactive	Active	Inactive
158950221	5000	Inactive	Inactive	Inactive	Inactive	Active	Inactive
89971570	5000	Inactive	Inactive	Inactive	Inactive	Active	Inactive
10086154	900	Inactive	Inactive	Inactive	Inactive	Active	Inactive
89095877	900	Inactive	Active	Inactive	Inactive	Active	Inactive
131841575	4800	Inactive	Inactive	Inactive	Inactive	Active	Inactive
118721173	4800	Inactive	Inactive	Inactive	Inactive	Active	Inactive
52921581	1624	Inactive	Inactive	Inactive	Inactive	Active	Inactive
73152384	5000	Inactive	Inactive	Inactive	Inactive	Active	Inactive
23243281	5000	Inactive	Active	Inactive	Inactive	Active	Inactive
10084402	2500	Inactive	Inactive	Inactive	Inactive	Active	Inactive
90074494	900	Inactive	Inactive	Inactive	Inactive	Active	Inactive
10336005	900	Inactive	Inactive	Inactive	Inactive	Active	Inactive
10563417	900	Inactive	Inactive	Inactive	Inactive	Active	Inactive

Compounds highlighted in red had at least 2 violations

Binding Affinity and Free Energy Analysis

Docking and MM-GBSA analyses revealed strong binding interactions for both receptors, with ZmPYL9 consistently exhibiting higher affinity ligands compared to ZmPYL12 (Tables 16 and 17). While compounds such as 15479571 and 166176980 demonstrated superior docking scores (≤ −10 kcal/mol), MM-GBSA analysis identified 10661840 as the most thermodynamically stable ZmPYL9 ligand, with a binding free energy of −96.18 kcal/mol (Table 16). Similarly, for ZmPYL12, compound 134611692 emerged as the top candidate, exhibiting the most favourable MM-GBSA value (−94.73 kcal/mol) despite moderate docking scores (Table 17). This highlights the importance of incorporating free energy calculations, which account for solvation effects and entropic contributions, thereby providing a more reliable estimation of ligand binding stability than docking alone (Genheden & Ryde, 2015). These results confirm that the identified compounds form highly stable protein-ligand complexes and reinforce their potential as functional ABA analogues.

Table 16: Binding Affinity and MM-GBSA Value of Top Performing Ligands for Zmpyl9

Pubchem ID	Docking Score (kcal/mol)	MM-GBSA (kcal/mol)
15479571	-10.498	-91.41
166176980	-10.223	-91.89
10379033	-9.755	-92.31
10514699	-9.671	-84.91
50909797	-9.641	-83.35
5280896	-9.533	-93.21
10588337	-9.533	-93.21
10661840	-9.394	-96.18
141813054	-9.195	-79.54
148240468	-9.015	-90.85
118646136	-8.880	-81.90
134553060	-7.988	-69.43

Table 17: Binding Affinity and MM-GBSA Value of Top Performing Ligands for Zmpyl12

Pubchem ID	Docking Score (kcal/mol)	MM-GBSA (kcal/mol)
134611692	-9.011	-94.73
158950221	-8.739	-87.54
5280896	-8.739	-87.54
90074494	-8.705	-63.98
10086154	-8.541	-73.09
162860100	-7.939	-66.89
10336005	-7.766	-72.69
118721173	-7.632	-83.06
131841575	-7.477	-72.28

Pubchem ID	Docking Score (kcal/mol)	MM-GBSA (kcal/mol)
52921581	-7.397	-66.02
73152384	-6.985	-71.99
10084402	-6.893	-64.69

Biological Implications

The PYR/PYL/RCAR receptor family plays a central role in ABA-mediated stress responses, including drought tolerance, stomatal regulation, and transcriptional reprogramming. The high structural conservation observed in ZmPYL9 and ZmPYL12 supports their functional roles as ABA receptors in maize. The identification of high-affinity ABA analogues, particularly 10661840 and 10588337 for ZmPYL9 and 134611692 for ZmPYL12, suggests strong potential for enhanced receptor activation and downstream signalling. Notably, the superior binding performance observed for ZmPYL9 indicates that it may serve as a more responsive target for ligand-mediated modulation, possibly due to subtle differences in binding pocket architecture or conformational dynamics.

These findings provide important insights into receptor-specific ligand selectivity and highlight opportunities for designing targeted agrochemicals to improve plant resilience under abiotic stress conditions.

CONCLUSION

This study established high-quality structural models of ZmPYL9 and ZmPYL12 and identified a diverse set of ABA-like ligands with strong binding affinity, favourable pharmacokinetic properties, and low toxicity. Integrative screening approaches revealed that compounds 10661840 and 10588337 are the most promising candidates for ZmPYL9, while compound 134611692 represents the leading ligand for ZmPYL12. It is worthy of note that ZmPYL9 demonstrated superior ligand-binding performance, highlighting its suitability as a primary target for agrochemical development. These findings therefore provide a robust computational framework for the rational design of ABA receptor agonists aimed at enhancing plant stress tolerance, with significant implications for sustainable agriculture and crop improvement.

REFERENCES

Al Azzam, K. M., Negim, E. S., & Aboul-Enein, H. Y. (2022). ADME studies of TUG-770 (a GPR-40 inhibitor agonist) for the treatment of type 2 diabetes using SwissADME predictor: In silico study. *Journal of Applied Pharmaceutical Science*, *12*(4), 159-169.

Banerjee, P., Eckert, A. O., Schrey, A. K., & Preissner, R. (2018). ProTox-II: A webserver for the prediction of toxicity of chemicals. *Nucleic Acids Research*, *46*(W1), W257–W263.

Bienert, S., Waterhouse, A., De Beer, T. A., Tauriello, G., Studer, G., Bordoli, L., & Schwede, T. (2017). The SWISS-MODEL Repository—new features and functionality. *Nucleic acids research*, *45*(D1), D313-D319.

Colovos, C., & Yeates, T. O. (1993). Verification of protein structures: Patterns of nonbonded atomic interactions. *Protein Science*, *2*(9), 1511–1519.

Daina, A., Michielin, O., & Zoete, V. (2017). SwissADME: A free web tool to evaluate pharmacokinetics, drug-likeness and medicinal chemistry friendliness of small molecules. *Scientific Reports*, *7*, 42717.

Driver, K. E., Brunharo, C. A., & Al-Khatib, K. (2020). Mechanism of clomazone resistance in Leptochloa fusca spp. fasicularis to clomazone. *Pesticide biochemistry and physiology*, *162*, 1-5.

Fidler, J., Graska, J., Gietler, M., Nykiel, M., Prabucka, B., Rybarczyk-Płońska, A., & Labudda, M. (2022). PYR/PYL/RCAR receptors play a vital role in the abscisic-acid-dependent responses of plants to external or internal stimuli. *Cells*, *11*(8), 1352.

Genheden, S., & Ryde, U. (2015). The MM/PBSA and MM/GBSA methods to estimate ligand-binding affinities. *Expert Opinion on Drug Discovery*, *10*(5), 449–461.

Melcher, K., Ng, L. M., Zhou, X. E., Soon, F. F., Xu, Y., Suino-Powell, K. M., & Xu, H. E. (2009). A gate–latch–lock mechanism for hormone signalling by abscisic acid receptors. *Nature*, *462*(7273), 602-608.

Park, S. Y., Fung, P., Nishimura, N., Jensen, D. R., Fujii, H., Zhao, Y., & Cutler, S. R. (2009). Abscisic acid inhibits PP2Cs via the PYR/PYL family of ABA-binding START proteins. *Science (New York, NY)*, *324*(5930), 1068.

Petrović, S., & Leskovac, A. (2026). Biopesticides and Human Health Risks: A Critical Review. *Toxics*, *14*(3), 246.

Pires, D. E., Blundell, T. L., & Ascher, D. B. (2015). pkCSM: predicting small-molecule pharmacokinetic and toxicity properties using graph-based signatures. *Journal of medicinal chemistry*, *58*(9), 4066-4072.

Sah, S. K., Reddy, K. R., & Li, J. (2016). Abscisic acid and abiotic stress tolerance in crop plants. *Frontiers in plant science*, *7*, 571.

Sharma, R., & Sharma, P. (2023). Role of Abscisic acid in plant stress. In *New insights into phytohormones*. IntechOpen.pp1-27

Studer, G., Rempfer, C., Waterhouse, A. M., Gumienny, R., Haas, J., & Schwede, T. (2020). QMEANDisCo—distance constraints applied on model quality estimation. *Bioinformatics*, *36*(6), 1765-1771.

Tian, W., Chen, C., Lei, X., Zhao, J., & Liang, J. (2018). CASTp 3.0: computed atlas of surface topography of proteins. *Nucleic acids research*, *46*(W1), W363-W367.

Tice, C. M. (2001). Selecting the right compounds for screening: does Lipinski's Rule of 5 for pharmaceuticals apply to agrochemicals?. *Pest Management Science: formerly Pesticide Science*, *57*(1), 3-16.

Waterhouse, A., Bertoni, M., Bienert, S., Studer, G., Tauriello, G., Gumienny, R., Heer, F. T., de Beer, T. A. P., Rempfer, C., Bordoli, L., Lepore, R., & Schwede, T. (2018). SWISS-MODEL: Homology modelling of protein structures and complexes. *Nucleic Acids Research*, *46*(W1), W296–W303.